Geochimica et Cosmochimica Acta 389 (2025) 211–223

Contents lists available at ScienceDirect

Geochimica et Cosmochimica Acta

journal homepage: www.elsevier.com/locate/gca

Stable and radiogenic strontium isotopes trace the composition and diagenetic alteration of remnant glacial seawater

Madison M. Wood [a,*], Clara L. Blättler [b], Ana Kolevica [c], Anton Eisenhauer [c], Adina Paytan [a]

[a] Department of Earth and Planetary Sciences, University of California, Santa Cruz, Santa Cruz, CA, 95064, USA
[b] Department of the Geophysical Sciences, University of Chicago, Chicago, IL, 60637, USA
[c] GEOMAR Helmholtz Centre for Ocean Research Kiel, 24148, Kiel, Germany

ARTICLE INFO

Associate editor: Claire Rollion-Bard

Dataset link: https://doi.org/10.17632/xs738ckr2m.1

Keywords:
Sr isotopes
Carbonate diagenesis
Glacial seawater

ABSTRACT

A remnant of glacial seawater preserved in the pore fluids of sediment cores from the Maldives Inner Sea provided an opportunity to investigate the stable strontium isotopic composition ($\delta^{88/86}$Sr) of the ocean during the Last Glacial Maximum and explore the usefulness of $\delta^{88/86}$Sr as a tracer of early marine diagenesis. We used paired measurements of $\delta^{88/86}$Sr and radiogenic Sr isotope ratios (^{87}Sr/^{86}Sr) in pore fluids and surrounding carbonate sediments to constrain the diagenetic history of the preserved glacial water mass at IODP Sites U1466 and U1468. These pore fluid profiles document variability in $\delta^{88/86}$Sr in a shallow marine setting, revealing distinct diagenetic processes dominating within different depth intervals. We find evidence for isotope fractionation during secondary calcite precipitation at intermediate depths and observe that in aragonite-dominated settings, fractionation during recrystallization may be obscured by the dissolution of aragonite in the uppermost sediments. Correcting for the effect of carbonate recrystallization on pore fluid Sr concentration ([Sr]) and isotopic composition, we estimate that glacial seawater [Sr] was higher (~ 98 μM) and $\delta^{88/86}$Sr lower (~0.32‰) compared to the modern ocean, consistent with hypotheses attributing the present-day disequilibrium of the ocean Sr budget to glacial/interglacial changes in shelf carbonate weathering and burial. Our results provide evidence that the ocean [Sr] and $\delta^{88/86}$Sr are sensitive to carbon cycle changes on timescales much shorter than its residence time (~2 Myr) and demonstrate that pore fluid $\delta^{88/86}$Sr measurements are a useful addition to multi-tracer studies of diagenesis in complex marine systems.

1. Introduction

Efforts to reconstruct glacial seawater chemistry predominantly rely on indirect proxy evidence in sediments or fossils that can be translated to the elemental and isotopic composition of the past ocean. Such reconstructions are inherently subject to uncertainties stemming from, for example, imperfect preservation of the sediment archives, biological or temperature effects, or assumptions of constant isotope fractionation through time. The discovery of a preserved remnant of Last Glacial Maximum (LGM) seawater in the interstitial fluids of a carbonate platform in the Maldives Inner Sea yielded a new archive from which geochemical properties of glacial seawater may be more directly derived (Blättler et al., 2019). The glacial-age pore fluids recovered by International Ocean Discovery Program Expedition 359 record increases in chloride concentrations, oxygen isotope ratios (δ^{18}O) and deuterium isotope ratios (δD) of 25 mM (4.5% change in chloride), 1.2‰, and 9‰, respectively, consistent with an LGM origin. Analyses of reactive geochemical tracers (strontium concentrations and calcium isotope ratios) revealed complex reactive histories for the water masses at these sites but suggest that the shallowest glacial pore fluids have been only minimally altered by reactions with the carbonate sediments (Figs. 1 and 2) (Blättler et al., 2019). These minimally-altered pore fluids offer a unique archive for investigating the chemical composition of seawater during the LGM.

The stable strontium isotopic composition ($\delta^{88/86}$Sr) of glacial seawater is of particular interest, as several studies have converged on the idea that non-steady-state processes operating over glacial/interglacial cycles drove imbalances in the strontium (Sr) budget and fluctuations in seawater $\delta^{88/86}$Sr (Krabbenhöft et al., 2010; Mokadem et al., 2015; Paytan et al., 2021; Pearce et al., 2015; Vance et al., 2009). The ocean Sr budget is presently not in chemical or isotopic equilibrium, implying perturbation from its long-term steady state (Davis et al., 2003; Krabbenhöft et al., 2010; Pearce et al., 2015; Vance et al., 2009). The rate of change in seawater radiogenic Sr isotope ratios (^{87}Sr/^{86}Sr) calculated based on modern fluxes is ~8 times faster than the observed

* Corresponding author.
E-mail address: mamwood@ucsc.edu (M.M. Wood).

https://doi.org/10.1016/j.gca.2024.10.028
Received 25 April 2024; Accepted 29 October 2024
Available online 9 November 2024

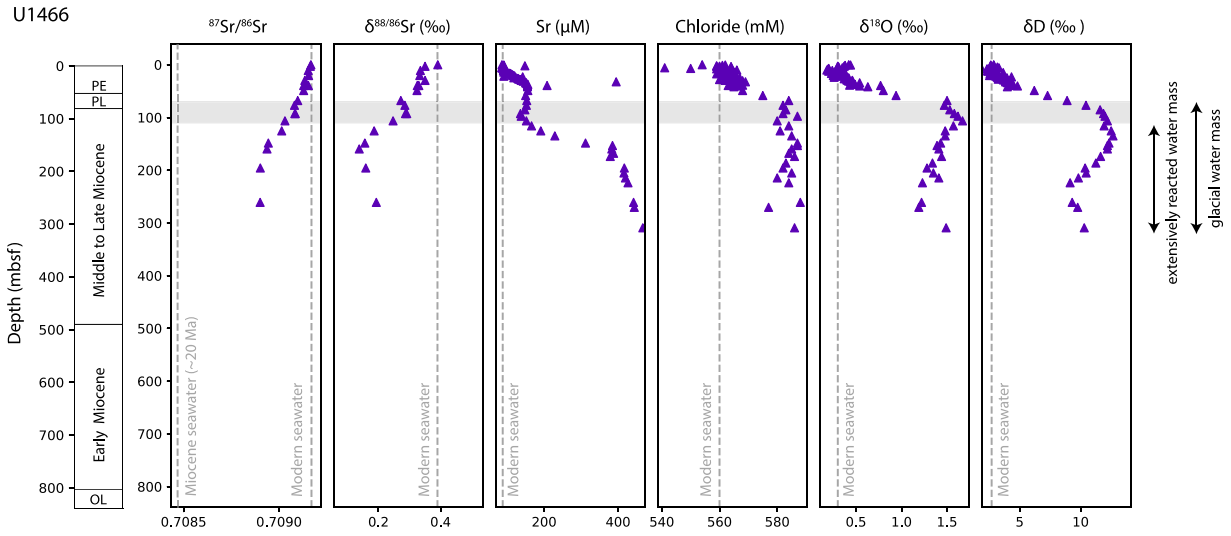

Fig. 1. Site U1466 pore fluid profiles of $^{87}Sr/^{86}Sr$ and $\delta^{88/86}Sr$ measured in this study, with published [Sr], chloride concentrations, $\delta^{18}O$, and δD profiles (Blättler et al., 2019). The best-preserved glacial interval (70 to 110 mbsf) is indicated by the shaded region and is defined based on the conservative tracers (chloride, $\delta^{18}O$, δD) and [Sr] as in Blättler et al. (2019). Modern seawater compositions and Early Miocene seawater $^{87}Sr/^{86}Sr$ are shown by the dashed vertical lines.

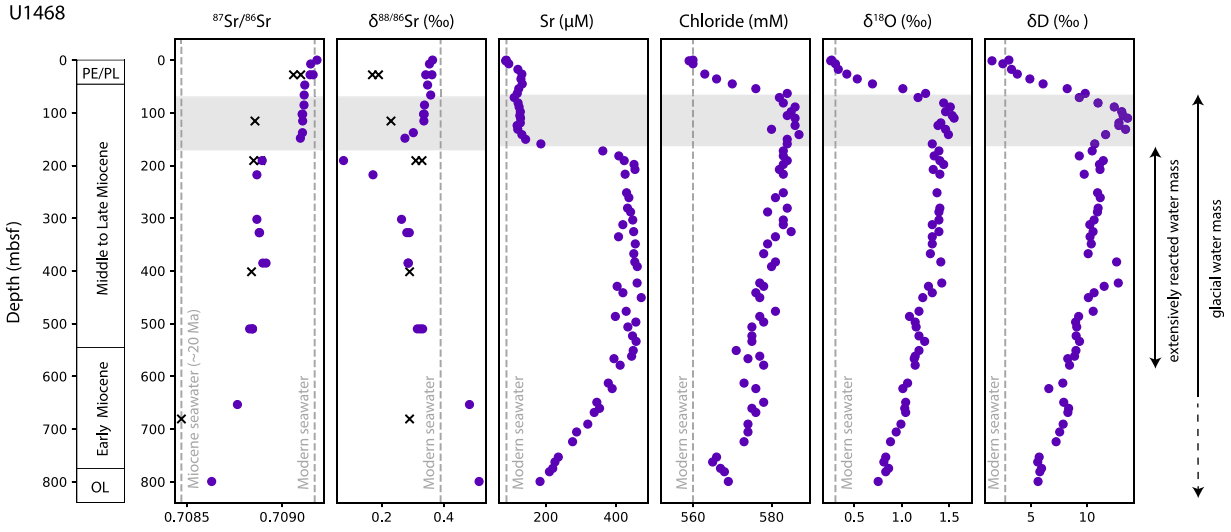

Fig. 2. Site U1468 pore fluid profiles of $^{87}Sr/^{86}Sr$ and $\delta^{88/86}Sr$ measured in this study, with published [Sr], chloride concentrations, $\delta^{18}O$, and δD profiles (Blättler et al., 2019). Bulk carbonate values at select depths are plotted as black "x" symbols. The best-preserved glacial interval (70 to 170 mbsf) is indicated by the shaded region and is defined based on the conservative tracers (chloride, $\delta^{18}O$, δD) and [Sr] as in Blättler et al. (2019). Modern seawater compositions and Early Miocene seawater $^{87}Sr/^{86}Sr$ are shown by the dashed vertical lines.

rate over the past few million years, suggesting high modern weathering rates relative to the long-term rate (Vance et al., 2009). However, a post-glacial increase in continental weathering cannot alone explain the modern isotopic disequilibrium of seawater $\delta^{88/86}Sr$; isotopic mass balance requires an additional source of isotopically light Sr, which may have been supplied by weathering and recrystallization of exposed shallow marine carbonate (aragonite) during the last glacial period (Krabbenhöft et al., 2010). The predicted equilibrium of the glacial Sr budget is thought to have been perturbed by sea level rise during deglaciation that cut off the carbonate weathering flux from the exposed continental shelf and increased the flooded shelf area available for shallow marine carbonate burial. Neritic aragonite deposits are rich in Sr with low $\delta^{88/86}Sr$ relative to seawater due to isotope fractionation during carbonate precipitation, so changes in shallow carbonate weathering and burial can influence both the ocean Sr inventory and $\delta^{88/86}Sr$ (Krabbenhöft et al., 2010; Pearce et al., 2015). In contrast, seawater $^{87}Sr/^{86}Sr$ is not sensitive to mass-dependent fractionation in carbonates and has been shown to be constant within analytical error over the last 40 kyr, limiting possible changes in continental weathering to less than 12% (Henderson et al., 1994; Mokadem et al., 2015). Combined constraints on glacial seawater $^{87}Sr/^{86}Sr$ and $\delta^{88/86}Sr$ could more fully characterize the glacial Sr budget and provide a new test of predicted glacial/interglacial changes in the shelf carbonate fluxes.

Previous work relying on numerical models predicted an increase in glacial seawater Sr concentration ([Sr]) due to the shelf recrystallization mechanism (Stoll and Schrag, 1998; Stoll et al., 1999), which holds important implications for the carbonate chemistry of the ocean and related changes in atmospheric carbon dioxide over glacial/interglacial cycles (Berger, 1982; Opdyke and Walker, 1992; Walker and Opdyke, 1995). The addition of Sr to the glacial ocean from recrystallizing shelf carbonates would also be expected to lower seawater $\delta^{88/86}Sr$ relative to the modern value if the flux was large enough to affect the ocean Sr inventory. Reduced aragonite burial on shelves during low stands would likewise lower seawater $\delta^{88/86}Sr$ by decreasing the preferential removal of isotopically light Sr from the ocean by carbonate precipitation. Limited data exist to constrain the

possible glacial increase in [Sr] (modeled by Stoll and Schrag (1998) as only a ~2% increase in Sr/Ca). The only published data for Pleistocene seawater $\delta^{88/86}$Sr, reconstructed using marine barite, indeed suggest that the average Late Quaternary seawater $\delta^{88/86}$Sr was ~0.04‰ lower than today, with the range in $\delta^{88/86}$Sr corresponding to a calculated ≤25% increase in [Sr] (Paytan et al., 2021). The Maldives pore fluid archive that is the focus of this study suggests the possibility that glacial seawater [Sr] could have been higher than today. The remnant LGM seawater [Sr] (~120 to 150 μM) is elevated compared to the modern concentration (88 μM). These higher concentrations could reflect some degree of carbonate recrystallization (Blättler et al., 2019) and possibly a higher Sr inventory in the glacial ocean associated with the shelf recrystallization hypothesis (Berger, 1982; Stoll and Schrag, 1998).

In order to utilize the Maldives pore fluids as an archive of glacial seawater chemistry, it is critical to correct for any alteration of the remnant LGM water mass through sediment–fluid reactions. The diagenesis of carbonate in contact with marine pore fluids can impart changes in pore fluid geochemistry, including [Sr] and the isotopes of Sr, calcium, and magnesium among other tracers (Fantle and DePaolo, 2007; Fantle et al., 2010; Fantle and Higgins, 2014; Geske et al., 2015; Higgins and Schrag, 2012; Higgins et al., 2018; Riechelmann et al., 2016). The effect of carbonate recrystallization on pore fluid $\delta^{88/86}$Sr in shallow marine sediments has not been studied, with only one previous study documenting these processes within deep-sea sediments (Voigt et al., 2015), but it is expected that the effect may be more substantial in shallow marine environments given the prevalence of Sr-rich aragonite, the much higher concentration of Sr in aragonite compared to pore fluids, and the fractionation of ^{88}Sr/^{86}Sr between carbonate and seawater (Fietzke and Eisenhauer, 2006; Krabbenhöft et al., 2010).

At the Maldives sites, Blättler et al. (2019) used both pore fluid [Sr] and calcium isotope ratios ($\delta^{44/40}$Ca) to identify depth intervals where the LGM water mass had been only minimally altered by carbonate recrystallization. The glacial origin of the water mass was determined based on its higher salinity and δ^{18}O and δD values (4.5%, 1.2‰ and 9‰ increases in chloride concentrations, δ^{18}O, and δD respectively, compared to modern seawater), while the extent of alteration was inferred from changes in [Sr] and $\delta^{44/40}$Ca with depth. Pore fluid [Sr] and $\delta^{44/40}$Ca were generally anti-correlated, evolving from the seawater endmember (high $\delta^{44/40}$Ca, low [Sr]) to a highly-altered fluid endmember with low $\delta^{44/40}$Ca and high [Sr] (Blättler et al., 2019). The main targets of our investigation are the glacial pore fluids that are least evolved with respect to $\delta^{44/40}$Ca and [Sr], which lie above sharp transitions to more evolved fluids at ~170 mbsf at Site U1468 and ~110 mbsf at Site U1466 (referred to hereafter as the "best-preserved glacial" intervals). However, we note that even a small degree of carbonate recrystallization can alter the pore fluid $\delta^{88/86}$Sr composition and must be accounted for. Pore fluid ^{87}Sr/^{86}Sr, which is often used as a tracer of carbonate recrystallization (Fantle and DePaolo, 2006; Fantle et al., 2010; Richter and DePaolo, 1987, 1988), constrains the extent of carbonate recrystallization at these sites and aids our interpretation of the pore fluid $\delta^{88/86}$Sr profiles. Our combined measurements of ^{87}Sr/^{86}Sr and $\delta^{88/86}$Sr provide new insight to the alteration of the best-preserved glacial water at Sites U1466 and U1468 and the effect of early marine diagenesis on pore fluid and carbonate $\delta^{88/86}$Sr.

We show that the best-preserved glacial seawater at the Maldives sites has been more extensively altered than previously inferred and that the contribution of carbonate recrystallization to the measured pore fluid Sr chemistry can be constrained using ^{87}Sr/^{86}Sr and [Sr], providing a means of estimating glacial seawater $\delta^{88/86}$Sr. These measurements of pore fluid $\delta^{88/86}$Sr in a shallow carbonate platform setting reveal distinct diagenetic processes dominating at different depth intervals and demonstrate the usefulness of pore fluid $\delta^{88/86}$Sr in multiple-tracer studies of complex carbonate systems.

2. Materials and methods

2.1. Site description and background

International Ocean Discovery Program Expedition 359 recovered sediment cores at eight sites including Site U1466 (4° 55.99'N, 73° 1.69'E, 518 m water depth) and Site U1468 (4° 55.98'N, 73° 4.28'E, 521 m water depth) in the Maldives Inner Sea, drilling into a drowned carbonate platform and overlying drift deposits of Miocene to Pleistocene age (Betzler et al., 2017). Measurements of conservative tracers (δ^{18}O, δD, chloride concentrations) and reactive tracers for carbonate recrystallization ([Sr], $\delta^{44/40}$Ca) in pore fluids extracted from these cores were used to identify the origin of advected water masses in the carbonate platform and their diagenetic histories (Blättler et al., 2019). The conservative tracer profiles were interpreted as reflecting distinct water masses of different ages: an interglacial (likely Holocene) water mass with δ^{18}O ≈ 0.3‰, δD ≈ 3‰, and chloride ≈ 559 μM (0 to ~60 mbsf) and a glacial water mass with δ^{18}O ≈ 1.5‰, δD ≈ 12‰, and chloride ≈ 584 μM (~70 to ~400 mbsf) (Blättler et al., 2019). Below 400 mbsf, the conservative tracers return to the interglacial seawater values. These pore fluid profiles revealed that the Maldives edifice uniquely stores glacial seawater hundreds of meters below the seafloor within host sediments that are millions of years older, due to lateral advection of water masses through the platform system (Blättler et al., 2019).

Non-conservative species in the Maldives pore fluids reflect diagenetic alteration in an open, advection-dominated system with a high water/rock ratio, distinct from typical pelagic sedimentary pore fluid profiles which are dominated by diffusion (e.g., Voigt et al., 2015). The profiles of [Sr] and $\delta^{44/40}$Ca generally reflect variable degrees of carbonate recrystallization (aragonite-to-calcite neomorphism and calcite-to-calcite recrystallization) at different depths and along the upstream advective paths of the fluids (Blättler et al., 2019). The conversion of Sr-rich aragonite to Sr-poor calcite releases Sr to pore fluids, while pore fluid $\delta^{44/40}$Ca decreases toward equilibrium with the sediments (which have lower $\delta^{44/40}$Ca than seawater due to the ~-1.0–1.5‰ average fractionation between precipitating carbonate and seawater) (Fantle and DePaolo, 2007; Fantle and Tipper, 2014; Turchyn and DePaolo, 2011). The reactive tracers shed light on the diagenetic histories of the water masses distinguished by the conservative tracers: the Holocene water mass remains largely unaltered by exchange with the sediments (0 to 60 mbsf), the uppermost glacial water mass (the best-preserved glacial interval) was interpreted as having minimal input of recrystallized carbonate (~70 to ~110 mbsf at Site U1466, ~70 to ~170 mbsf at Site U1468), and the deeper glacial water mass has undergone extensive reaction with carbonate sediments (> 110 mbsf at Site U1466, > 170 mbsf at Site U1468) (Blättler et al., 2019) (Figs. 1 and 2).

2.2. Sample selection

We analyzed ^{87}Sr/^{86}Sr and $\delta^{88/86}$Sr in pore fluids sampling the distinct Holocene and glacial water masses identified by Blättler et al. (2019) at Sites U1466 and U1468 (Table 1). We sampled coarsely throughout the depth intervals of pore fluid recovery (maximum recovery depths of 309 mbsf and 838 mbsf at Site U1466 and Site U1468, respectively). Selected samples from Site U1466 span depths of 0 to 261 mbsf while samples from Site U1468 reach up to 799 mbsf, though we focused mainly in the upper 300 m. Pore fluid recovery was limited by lithification at greater depths. The pore fluids in the sampled intervals are primarily within Miocene carbonate sediments, with Pleistocene/Pliocene drift deposits in the upper 50 to 70 m (Betzler et al. 2018). Five carbonate samples from Site U1468 spanning 30 to 680 mbsf were also analyzed to characterize the Sr isotopic composition of the sediments in contact with the pore fluids (Table 2).

Table 1
Pore fluid Sr isotope measurements at Site U1466 and Site U1468 with internal precision given by $2\sigma_{mean}$. Asterisks indicate preparation replicate samples.

Site	Hole	Core	Type	Sect	Depth (mbsf)	$\delta^{88/86}$Sr	$2\sigma_{mean}$	n	$^{87}Sr/^{86}Sr$	$2\sigma_{mean}$
U1466	A	1	H	1	0	0.391	0.009	4	0.709167	0.000006
U1466	A	1	H	2	2.96	0.350	0.009	4	0.709164	0.000010
U1466	A	2	H	4	10.96	0.335	0.002	4	0.709153	0.000008
U1466	A	3	H	4	20.45	0.333	0.003	4	0.709155	0.000001
U1466	A	4	H	4	29.74	0.350	0.003	2	0.709135	0.000003
U1466	A	5	H	4	39.4	0.325	0.000	2	0.709129	0.000004
U1466	A	5	H	4	39.4*	0.330	0.004	4	0.709154	0.000010
U1466	A	6	H	4	48.9	0.324	0.008	2	0.709129	0.000009
U1466	A	8	H	4	67.9	0.272	0.006	2	0.709098	0.000014
U1466	A	9	H	4	76.9	0.285	0.006	4	0.709081	0.000007
U1466	A	11	H	4	92.6	0.287	0.009	4	0.709085	0.000004
U1466	A	11	H	4	92.6*	0.291	0.004	4	0.709083	0.000008
U1466	A	13	H	4	106.4	0.247	0.005	4	0.709031	0.000001
U1466	A	15	H	4	125.4	0.186	0.002	4	0.709014	0.000001
U1466	A	19	F	2	148.5	0.156	0.002	4	0.708944	0.000001
U1466	A	21	H	4	159.68	0.138	0.006	4	0.708937	0.000004
U1466	A	28	F	2	195.81	0.159	0.006	2	0.708902	0.000003
U1466	A	40	F	2	261	0.193	0.004	4	0.708901	0.000002
U1468	A	1	H	1	0	0.364	0.009	4	0.709182	0.000005
U1468	A	2	H	3	7.4	0.354	0.005	2	0.709149	0.000004
U1468	A	4	H	4	27.85	0.362	0.005	4	0.709162	0.000009
U1468	A	4	H	4	27.85*	0.342	0.014	4	0.709146	0.000001
U1468	A	6	H	4	47.35	0.348	0.009	4	0.709118	0.000002
U1468	A	8	H	4	66.3	0.358	0.003	4	0.709115	0.000001
U1468	A	10	H	4	85.3	0.338	0.003	4	0.709114	0.000004
U1468	A	12	H	4	102.65	0.335	0.003	2	0.709104	0.000005
U1468	A	12	H	4	102.65*	0.337	0.009	4	0.709107	0.000002
U1468	A	14	F	2	115.5	0.336	0.001	2	0.709107	0.000001
U1468	A	20	F	2	137.7	0.302	0.006	4	0.709106	0.000002
U1468	A	22	F	2	148.2	0.275	0.006	4	0.709095	0.000007
U1468	A	30	F	2	190.6	0.077	0.005	4	0.708895	0.000004
U1468	A	37	F	1	217.6	0.172	0.001	4	0.708867	0.000001
U1468	A	48	F	1	302.1	0.264	0.003	4	0.708867	0.000006
U1468	A	53	X	2	327.35	0.281	0.002	4	0.708879	0.000006
U1468	A	53	X	2	327.35*	0.289	0.001	4	0.708881	0.000005
U1468	A	61	X	4	385.1	0.285	0.025	4	0.708915	0.000002
U1468	A	61	X	4	385.1*	0.286	0.006	4	0.708898	0.000010
U1468	A	74	X	3	509.91	0.315	0.009	4	0.708844	0.000006
U1468	A	74	X	3	509.91*	0.332	0.001	4	0.708829	0.000001
U1468	A	74	X	3	509.91*	0.324	0.008	4	0.708844	0.000002
U1468	A	89	X	2	653.42	0.483	0.006	4	0.708765	0.000008
U1468	A	104	X	2	799.41	0.514	0.001	4	0.708630	0.000004

Table 2
Carbonate Sr isotope measurements at Site U1468 with internal precision given by $2\sigma_{mean}$. Asterisks indicate preparation replicate samples.

Site	Hole	Core	Type	Sect	Depth (mbsf)	$\delta^{88/86}$Sr	$2\sigma_{mean}$	n	$^{87}Sr/^{86}Sr$	$2\sigma_{mean}$
U1468	A	4	H	4	27.9	0.170	0.018	4	0.709097	0.000006
U1468	A	4	H	4	27.9*	0.190	0.016	4	0.709059	0.000002
U1468	A	14	F	2	115.6	0.230	0.011	4	0.708857	0.000010
U1468	A	30	F	2	190.7	0.310	0.007	4	0.708888	0.000007
U1468	A	30	F	2	190.7*	0.330	0.004	4	0.708850	0.000001
U1468	A	63	X	2	401.6	0.290	0.007	4	0.708839	0.000006
U1468	A	92	X	1	680.79	0.290	0.005	4	0.708471	0.000001

2.3. Sample preparation

Pore fluids were extracted shipboard by standard methods as reported in Blättler et al. (2019). We processed carbonate samples from squeeze cake bulk sediments according to a carbonate leaching method where approximately 100 mg of powdered sample was weighed into acid washed 50 mL centrifuge tubes. Samples were rinsed three times with ultrapure water to remove water-soluble Sr from ion-exchange sites, shaken and centrifuged, and the supernatant was decanted. The carbonate was dissolved using triple-distilled 0.75N HCl which was briefly reacted with the sample, centrifuged, and decanted. Pore fluids and dissolved carbonates were measured for elemental composition by inductively coupled plasma optical emission spectrometry and the resulting [Sr] of each sample was used to determine the amount of $^{87}Sr/^{84}Sr$ spike to be added to a volume containing 600 ng Sr. Strontium from both spiked and un-spiked (used to measure $^{87}Sr/^{86}Sr$) aliquots was purified using Eichrom's Sr-Spec stick/non-stick resin on 1 mL Bio-Rad columns (Krabbenhöft et al., 2009, 2010). Following cleaning and conditioning steps, the sample was loaded onto the column and washed with 5 mL of triple-distilled 8N HNO_3 before Sr was eluted with 7 mL of triple-distilled 0.05N HNO_3. Procedural Sr blanks for the carbonate leaching and column procedures were < 1.5 ng and < 0.5 ng, respectively, which are sufficiently low for the sample size prepared (< 0.3%).

2.4. Sr isotope analyses

Radiogenic and stable Sr isotope analyses were carried out at GEOMAR-Helmholtz Center for Ocean Research Kiel (Germany) using the double-spike thermal ionization mass spectrometry (DS-TIMS) method detailed by Krabbenhöft et al. (2009). In short, approximately

600 ng Sr was loaded onto degassed rhenium filaments with a tantalum activator, dried, and heated briefly at 2 A before loading on the TIMS. A single measurement requires separate analyses of an $^{87}Sr/^{84}Sr$-spiked sample and an unspiked sample, from which the $^{88}Sr/^{86}Sr$ ratios were calculated by the double spike correction algorithm and reported in delta notation as $\delta^{88/86}Sr$ (‰) = ($^{88}Sr/^{86}Sr_{sample}$/ $^{88}Sr/^{86}Sr_{SRM987}$ - 1) * 1000. We report the traditional radiogenic Sr isotope value $^{87}Sr/^{86}Sr$ normalized to a $^{88}Sr/^{86}Sr$ ratio of 8.375209. The typical internal precision for an individual measurement is < 0.00001 for $^{87}Sr/^{86}Sr$ and < 0.01 for $^{88}Sr/^{86}Sr$ (shown in Tables 1 and 2). The external reproducibility, which fully captures the variability introduced by the chemical preparation, was determined by repeated measurements of the JCp-1 coral standard ($\delta^{88/86}Sr$ =0.191 ± 0.015‰, $^{87}Sr/^{86}Sr$,=0.70918 ± 0.00002, n=9), the IAPSO seawater standard ($\delta^{88/86}Sr$ =0.389 ± 0.013‰, $^{87}Sr/^{86}Sr$,=0.709174 ± 0.000007, n=10), and NIST SRM 987 ($\delta^{88/86}Sr$ =0.003 ± 0.016‰, $^{87}Sr/^{86}Sr$,=0.71026 ± 0.00002, n=6) separately processed by Sr-Spec chromatography.

3. Results

3.1. Pore fluid $\delta^{88/86}Sr$ and $^{87}Sr/^{86}Sr$

At Site U1466, pore fluid [Sr] in the upper 10 meters of the core is similar to modern seawater (88 μM), increasing to ~150 μM between 10 and 30 mbsf (Fig. 1). Below 110 meters depth, [Sr] rapidly increases to greater than ~400 μM. The $\delta^{88/86}Sr$ profile shows opposing shifts to [Sr] with depth, decreasing from 0.4‰ at the core top to 0.33‰ over the upper 20 meters and maintaining this value until about 50 meters depth. Between 100 and 160 mbsf, $\delta^{88/86}Sr$ rapidly decreases to a minimum value of 0.14‰ as [Sr] increases. Below 160 mbsf, $\delta^{88/86}Sr$ increases back to 0.19‰ in the deepest sample. Radiogenic Sr decreases with depth from 0.709167 to 0.708901, with the greatest shift in $^{87}Sr/^{86}Sr$ occurring between 70 and 160 meters depth (0.709081 to 0.708937).

Site U1468 pore fluids exhibit similar trends but differ significantly from the Site U1466 profiles within the best-preserved glacial interval (70–170 mbsf) and extend to greater depths (Fig. 2). Strontium concentrations increase from 87 μM to 130 μM in the upper 30 meters and plateau until below 150 mbsf. Between 150 and 500 mbsf, [Sr] reaches 450 μM before decreasing from 400μM to ~220 μM between 500 and 800 mbsf. The $\delta^{88/86}Sr$ values show considerably less variation within the upper 150 meters compared to the Site U1466 profile, gradually decreasing from 0.36 to 0.34‰ between 0 and 120 mbsf, to 0.28‰ at ~150 mbsf. The $\delta^{88/86}Sr$ minimum (0.08‰) is reached at 190 meters before $\delta^{88/86}Sr$ begins increasing to a maximum value of 0.51‰ at 800 mbsf. As at Site U1466, pore fluid $^{87}Sr/^{86}Sr$ at Site U1468 decreases with depth but does so much more gradually between 0–150 mbsf (0.709182 to 0.709095). The pore fluid $^{87}Sr/^{86}Sr$ values are more radiogenic (higher) than the bulk carbonate values, most significantly so in the 70–170 mbsf depth interval and around 700 mbsf. Below 150 mbsf, Site 1468 $^{87}Sr/^{86}Sr$ values are similar to those at comparable depths at Site U1466.

Cross plots of [Sr] versus $^{87}Sr/^{86}Sr$ and $\delta^{88/86}Sr$ illustrate the trends that are broadly shared between the two sites and highlight some key differences (Fig. 3). Both sites show generally decreasing $^{87}Sr/^{86}Sr$ with increasing [Sr] at depths shallower than 400 mbsf. Site U1466 exhibits a deviation from this trend where [Sr] values remain mostly constant (~150 μM) while $^{87}Sr/^{86}Sr$ values decrease from ~0.70915 to ~0.70903, in contrast to Site U1468 where $^{87}Sr/^{86}Sr$ values decrease by only about half as much during the plateau in [Sr] between ~30 to 150 mbsf. At greater depths (Site U1468 only), the negative relationship between [Sr] and $^{87}Sr/^{86}Sr$ is reversed, with [Sr] decreasing while $^{87}Sr/^{86}Sr$ values continue to decrease. In [Sr] versus $\delta^{88/86}Sr$ space, $\delta^{88/86}Sr$ values also generally decrease with increasing [Sr] in the shallower depths sampled at both sites (0 to 400 mbsf), with similar structures to the $^{87}Sr/^{86}Sr$ vs. [Sr] plots around the 130–150 μM [Sr] plateau. At both sites, $\delta^{88/86}Sr$ values reach a minimum around 400 μM [Sr], shifting back to higher values as [Sr] increases in deeper samples (~200 mbsf). Below ~400 mbsf (Site U1468 only), the relationship between $\delta^{88/86}Sr$ and [Sr] is again negative, but shifted to significantly higher $\delta^{88/86}Sr$ values above even that for modern seawater.

3.2. Bulk carbonate $\delta^{88/86}Sr$ and $^{87}Sr/^{86}Sr$

Bulk carbonate measurements at Site U1468 yielded $\delta^{88/86}Sr$ and $^{87}Sr/^{86}Sr$ values of 0.17 to 0.33‰ and 0.708471 to 0.709097, respectively (Fig. 2). The Pleistocene/Pliocene carbonate sediments in the upper part of the core (< 50 mbsf) are characterized by more radiogenic $^{87}Sr/^{86}Sr$ (0.709078) compared to the deeper Miocene sediments as expected based on the global seawater $^{87}Sr/^{86}Sr$ curve (McArthur et al., 2020). Carbonate $^{87}Sr/^{86}Sr$ values between 100 and 400 mbsf range from 0.708839 to 0.708888 (~10–12 Ma, McArthur et al. (2020)), while the deepest carbonate sample at 680 mbsf has the least radiogenic $^{87}Sr/^{86}Sr$ value of 0.708471 (~19.6 Ma, McArthur et al. (2020)). The lowest carbonate $\delta^{88/86}Sr$ is 0.18‰ in the Pleistocene/Pliocene sediments, generally consistent with the 0.15 to 0.21‰ range estimated for marine carbonates (Pearce et al., 2015; Krabbenhöft et al., 2010). The late Miocene carbonate sample at 115.6 mbsf has a $\delta^{88/86}Sr$ value of 0.23‰, with higher $\delta^{88/86}Sr$ values in the older, deeper sediments (0.29 to 0.33‰).

4. Discussion

4.1. Alteration of remnant glacial seawater

Our $^{87}Sr/^{86}Sr$ measurements show that the pore fluids in the intervals defined as best-preserved glacial seawater which were expected to record glacial seawater $\delta^{88/86}Sr$ have experienced enough alteration to influence the pore fluid radiogenic Sr isotopes. Pore fluid $^{87}Sr/^{86}Sr$ provides a key constraint on recrystallization at these sites because the $^{87}Sr/^{86}Sr$ of the glacial ocean is known to be within analytical error of the modern value (Henderson et al., 1994; Mokadem et al., 2015). Reconstructed from measurements of glacial-age planktonic foraminifera, the average glacial seawater $^{87}Sr/^{86}Sr$ was 0.7091784 ± 0.0000035, compared to the average modern seawater value of 0.7091792 ± 0.0000021 obtained by sampling the major oceans (Atlantic, Pacific, Indian, and the Labrador Sea) (Mokadem et al., 2015). Within the best-preserved glacial pore fluid interval at Site U1468 (70–170 mbsf), the shift in pore fluid $^{87}Sr/^{86}Sr$ values away from the expected seawater composition indicates addition of Sr with lower $^{87}Sr/^{86}Sr$ from the surrounding carbonates, which will also have influenced [Sr] and the stable Sr isotopic composition of the pore fluids (Fig. 2). The glacial pore fluids at Site U1466 (70–110 mbsf) appear even more altered, as $^{87}Sr/^{86}Sr$ values decrease rapidly with depth (Fig. 1). Since seawater $^{87}Sr/^{86}Sr$ during the LGM was indistinguishable (within analytical error) from the modern ocean composition, we would expect both the glacial pore fluids and the overlying Holocene pore fluids to have $^{87}Sr/^{86}Sr$ values identical to that of modern seawater in the absence of diagenetic alteration. Instead, the observed shift of pore fluid $^{87}Sr/^{86}Sr$ away from the modern seawater value to increasingly lower values with depth indicates that interaction with older, lower-$^{87}Sr/^{86}Sr$ carbonate sediments has altered pore fluid Sr at both sites.

Alteration of the best-preserved glacial pore fluids by carbonate recrystallization is consistent with the pore fluid $\delta^{44/40}Ca$ profiles published by Blättler et al. (2019), which decrease to values lower than the modern seawater composition within the depth interval of the best-preserved glacial seawater. Lower $\delta^{44/40}Ca$ values are indicative of carbonate recrystallization, which shifts pore fluid $\delta^{44/40}Ca$ toward equilibrium with the lower-$\delta^{44/40}Ca$ solid (Fantle and DePaolo, 2007), supporting the interpretation that Sr has been added to the best-preserved glacial pore fluids by diagenesis. This result does not rule out the possibility that there may be true differences in LGM seawater [Sr]

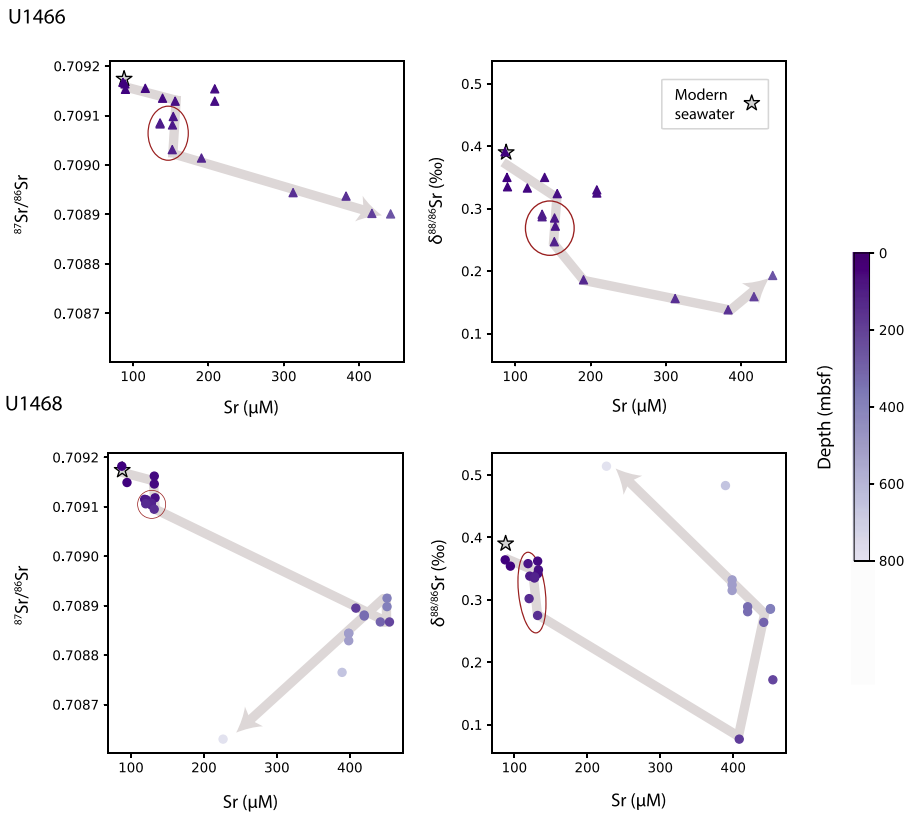

Fig. 3. Crossplots of pore fluid $^{87}Sr/^{86}Sr$ and $\delta^{88/86}Sr$ versus [Sr] at Site U1466 (top) and U1468 (bottom). Gray arrows provide a visual guide for changes with depth. Red outlines indicate samples that fall within the best-preserved glacial depth intervals defined by conservative tracers as described in the text and by Blättler et al. (2019).

or $\delta^{88/86}Sr$ compared to modern, but does confirm that the higher [Sr] in the best-preserved glacial pore fluid compared to modern seawater is at least partially due to the contributions from carbonate recrystallization, which will also impact pore fluid $\delta^{88/86}Sr$. Thus, neither of these tracers in the Maldives pore fluids can be defined as representing unaltered glacial seawater values but must instead be corrected for the effect of carbonate recrystallization, which will impact Sr but will not have an effect on conservative tracers such as $\delta^{18}O$, δD, and chloride concentrations.

4.2. Estimating glacial seawater [Sr] and $\delta^{88/86}Sr$

4.2.1. Mass balance of carbonate input to pore fluids

We used our pore fluid and bulk carbonate $^{87}Sr/^{86}Sr$ measurements to constrain the contribution of Sr from the sediments to the best-preserved glacial pore fluids. Since the $^{87}Sr/^{86}Sr$ of the glacial ocean is known, the recrystallized carbonate input to the glacial water mass can be determined by mass balance, which can then be used to calculate the $\delta^{88/86}Sr$ of the remnant LGM seawater. As a first approximation we assumed that the measured pore fluid [Sr] and isotopic composition resulted from the addition of recrystallized input from surrounding carbonates to the glacial seawater end-member with negligible diffusion. We neglect the potential for diffusive mixing of the fluid end-members in the system (Holocene water, best-preserved glacial water, and highly altered pore fluid) and treat the best-preserved glacial interval as an isolated water mass altered only by reaction with the surrounding sediments. Based on the sharp transitions in some of the pore fluid Sr and $\delta^{44/40}Ca$ profiles, we expect that vertical diffusive mixing was minimized by stratigraphic permeability barriers (Blättler et al., 2019). We recognize the uncertainty of potential upstream reactions with sediments along the advective flow path which could have different mineralogy, [Sr], age, and $^{87}Sr/^{86}Sr$ than the carbonate sediments recovered in the cores, so we use the core sediment composition as a starting point, but also perform calculations across a range of possible carbonate $^{87}Sr/^{86}Sr$ values.

Mass balance of the glacial seawater and recrystallized carbonate end member contributions to the pore fluid is described by:

$$[Sr]_{pf} * V_{pf} = [Sr]_{gsw} * V_{pf} + m_x \quad (1)$$

where V_{pf} is the pore fluid unit volume (V_{pf} = 1 L). The pore fluid Sr concentration ($[Sr]_{pf}$) is known, while the concentration of glacial seawater Sr ($[Sr]_{gsw}$) and the mass of Sr added by carbonate recrystallization (m_x) are unknown variables.

We solved for $[Sr]_{gsw}$ and m_x using the additional constraint of the radiogenic Sr isotopic mass balance:

$$[Sr]_{pf} * V_{pf} * F_{pf} = [Sr]_{gsw} * V_{pf} * F_{gsw} + m_x * F_x \quad (2)$$

The fractional isotopic abundance ($F = {}^{87}Sr/^{86}Sr$ / (1 + $^{87}Sr/^{86}Sr$)) of glacial seawater (F_{gsw}) is constrained by the reconstructed glacial seawater $^{87}Sr/^{86}Sr$ value (0.7091784, Mokadem et al. (2015)). We determined the pore fluid fractional isotopic abundance (F_{pf}) from our measurements of pore fluid $^{87}Sr/^{86}Sr$ and we used our carbonate $^{87}Sr/^{86}Sr$ measurements to constrain the recrystallized input composition (F_x), assuming that all recrystallization adds Sr to pore fluids and is represented by the m_x term (that is, there is negligible Sr isotopic exchange). First, we assumed that the measured $^{87}Sr/^{86}Sr$ of the bulk carbonate in the surrounding core sediment is representative of the recrystallized input $^{87}Sr/^{86}Sr$. We solved Eqs. (1) and (2) for each pore fluid sample within the best-preserved glacial intervals at both sites (11 samples total including two procedural replicates) using the composition of the carbonate sediments within the best-preserved glacial interval (Late Miocene-age, $^{87}Sr/^{86}Sr$ = 0.708857, F_x = 0.414814) (Table 3). We then evaluated the uncertainty associated with this assumption (e.g., the possibility of upstream reactions with sediments of a different age and $^{87}Sr/^{86}Sr$) by solving for $[Sr]_{gsw}$ and m_x as a

Table 3
Mass balance solutions for the recrystallized Sr mass added to the pore fluids (m_x) and glacial seawater Sr concentration ($[Sr]_{gsw}$) assuming a recrystallized input $^{87}Sr/^{86}Sr$ value equal to the composition of the surrounding Late Miocene carbonate sediments (0.708857). Asterisks indicate preparation replicate samples.

Site	Depth (mbsf)	$[Sr]_{pf}$ (μM)	F_{pf}	m_x (μmol)	Recrystallized contribution (%)	$[Sr]_{gsw}$ (μM)
U1466	67.9	153	0.414896	38	25	115
U1466	76.9	152	0.414890	46	30	106
U1466	92.6	136	0.414892	39	29	96
U1466	92.6*	136	0.414891	40	30	95
U1466	106.4	152	0.414873	70	46	82
U1468	85.3	121	0.414902	24	20	97
U1468	102.65	127	0.414898	30	23	98
U1468	102.65*	127	0.414899	28	22	99
U1468	115.5	128	0.414899	28	22	100
U1468	137.7	120	0.414899	27	23	93
U1468	148.2	132	0.414895	34	26	98

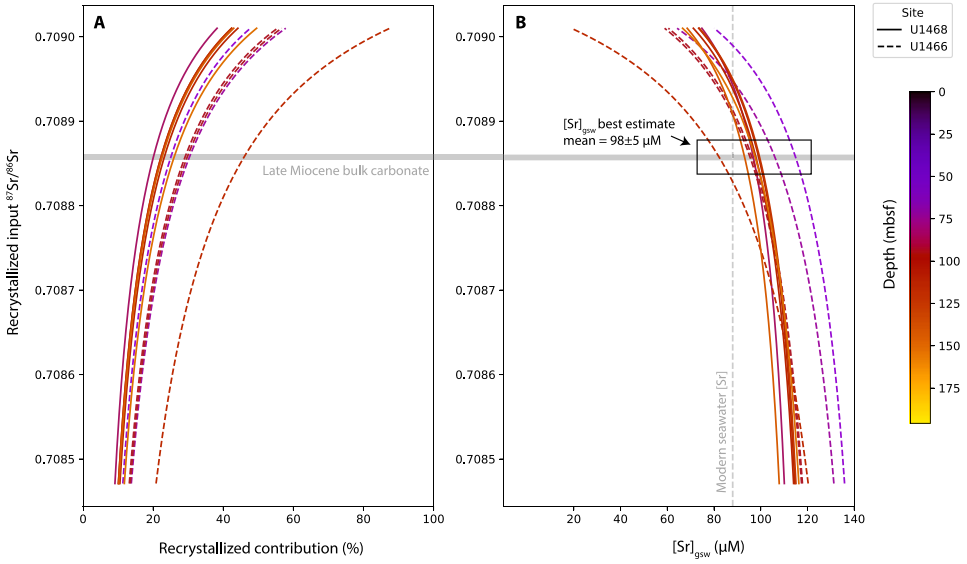

Fig. 4. Mass balance solutions for (A) the recrystallized Sr contribution to the pore fluids and (B) glacial seawater Sr concentration ($[Sr]_{gsw}$) as a function of the recrystallized input $^{87}Sr/^{86}Sr$ (F_x) as described in Section 4.2.1. For a given value of F_x (y-axis), Eqs. (1) and (2) are solved simultaneously to yield the percent contribution from recrystallization and $[Sr]_{gsw}$ (x-axes). Continuous solutions for each pore fluid sample across the range of possible F_x values are shown by solid (Site U1468) and dashed (Site U1466) lines with colors indicating sample depth in the core. Discrete solutions computed assuming recrystallized input $^{87}Sr/^{86}Sr$ equal to the composition of the surrounding Late Miocene carbonate sediments (0.708857, shown with horizontal gray line) are also displayed in Table 3.

function of F_x, allowing the assumed recrystallized input $^{87}Sr/^{86}Sr$ to vary within the range measured for the Pleistocene (0.709097) to Early Miocene (0.708471) bulk carbonates (Fig. 4).

For a value of F_x equal to the surrounding Late Miocene carbonate composition, we found that recrystallized input contributed 24–70 μmol Sr (20%–46% of the pore fluid unit volume Sr) (Table 3, Fig. 4A). The recrystallized input requires dissolution of only a very small mass of aragonite sediment (< 1 g). While this minimal degree of recrystallization is sufficient to alter [Sr] and the Sr isotopic composition of the pore fluids, the effect on the carbonate Sr composition would be negligible given the much greater Sr content of aragonite compared to seawater. For lower values of recrystallized input $^{87}Sr/^{86}Sr$, representing possible upstream reactions with older carbonate sediments with lower $^{87}Sr/^{86}Sr$ values, the recrystallized contribution is smaller (as low as 11–32 μmol for recrystallized input with Early Miocene bulk carbonate $^{87}Sr/^{86}Sr = 0.708471$). Increased recrystallization would be required if the pore fluids reacted with Pleistocene/Pliocene carbonate sediments with $^{87}Sr/^{86}Sr$ more similar to seawater (Fig. 4A); this scenario may be more likely given decreased reactivity of carbonate sediments with increasing age (Richter and DePaolo, 1988) but the majority of the sediments at these sites are Miocene-age with Pleistocene/Pliocene carbonate sediments limited to the upper ~50–70 m. We attribute the variability in our solutions for any given F_x to distinct reactive histories for each pore fluid sample. The pore fluid profiles for these sites demonstrate complex variation both laterally and with depth over relatively short spatial scales (Blättler et al., 2019). Therefore the composition of the recrystallized input may vary between the two sites and between pore fluid samples within a given depth range at the same site.

Assuming recrystallized input only from the surrounding sediments ($^{87}Sr/^{86}Sr = 0.708857$, carbonate age ~11 Ma based on the Sr isotope stratigraphy by McArthur et al. (2020)), our solutions give a mean Sr concentration of glacial seawater of 98 ± 5 μM (95% CI) (Fig. 4B). This best estimate is ~10% higher than the modern seawater [Sr] and aligns with Paytan et al.'s (2021) calculated change in Pleistocene seawater (up to 25% higher than the modern concentration of 88 μM). For lower values of recrystallized input $^{87}Sr/^{86}Sr$, the predicted glacial seawater [Sr] increases up to an average of 118 ± 5 μM (recrystallized input $^{87}Sr/^{86}Sr = 0.708471$, carbonate age ~20 Ma). Interaction with sediments younger than ~8 Ma (recrystallized input $^{87}Sr/^{86}Sr > 0.70893$) produces average glacial seawater [Sr] solutions similar to or lower than the modern ocean [Sr]. In summary, the hypothesis that the glacial ocean had a higher Sr inventory than the modern ocean is supported for cases where the recrystallized input $^{87}Sr/^{86}Sr$ is less than ~0.70893, corresponding to recrystallizing sediment ages older than ~8 Ma. Given that the Maldives carbonate platform sediments are mainly Miocene, with younger drift deposits only in the upper ~50–70 m at Sites U1466 and U1468 (Betzler et al., 2017, 2018), the glacial pore fluids likely

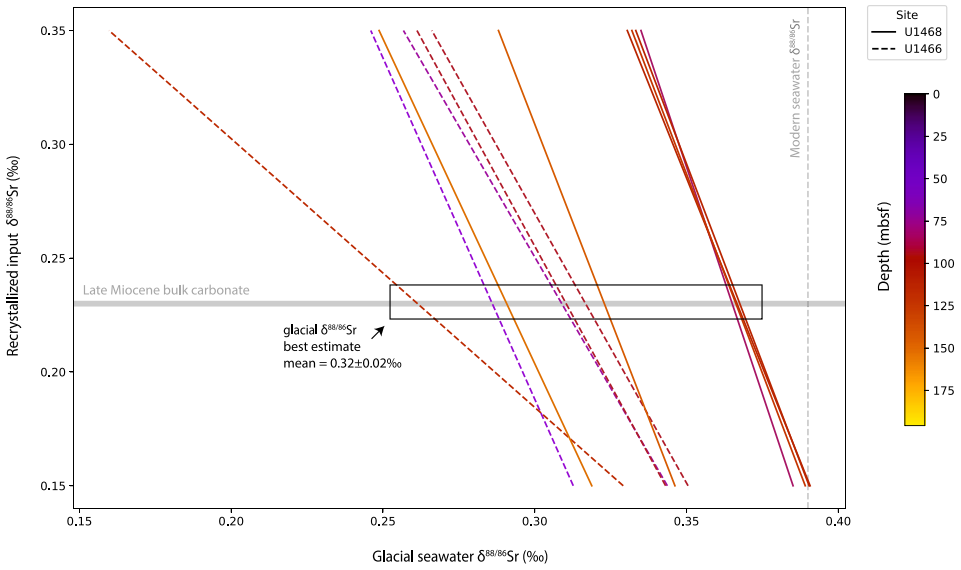

Fig. 5. Mass balance solutions for glacial seawater $\delta^{88/86}$Sr (δ_{gsw}) calculated using Eq. (3). Continuous solutions for each pore fluid sample across the range of possible recrystallized input $\delta^{88/86}$Sr (δ_x) values are shown by solid (Site U1468) and dashed (Site U1466) lines with colors indicating sample depth in the core. All solutions assume a recrystallized input ^{87}Sr/^{86}Sr (F_x) value equal to the ^{87}Sr/^{86}Sr of the surrounding carbonates (0.708857) as described in Section 4.2.2. The $\delta^{88/86}$Sr of the surrounding Late Miocene carbonates (0.23‰) is indicated by the gray horizontal line.

interacted with the older (> 8 Ma) sediments, though the flow patterns for this system remain speculative (Blättler et al., 2019) and exchange rates decrease as carbonate sediments age (Richter and DePaolo, 1988).

4.2.2. Stable Sr isotopic mass balance

We used the F_x-dependent solutions for m_x and $[Sr]_{gsw}$ to solve the stable Sr isotopic mass balance (Eq. (3)) and estimate glacial seawater $\delta^{88/86}$Sr (δ_{gsw}).

$$[Sr]_{pf} * V_{pf} * \delta_{pf} = [Sr]_{gsw} * V_{pf} * \delta_{gsw} + m_x * \delta_x \quad (3)$$

The $\delta^{88/86}$Sr of the pore fluids (δ_{pf}) is known from our measurements. As before, we took the composition of the surrounding Late Miocene carbonates ($\delta^{88/86}$Sr = 0.23‰, ^{87}Sr/^{86}Sr = 0.708857) to be representative of the recrystallized input composition (δ_x, F_x) while also solving across a range of δ_x values to evaluate the sensitivity of our δ_{gsw} solutions to this assumption (Fig. 5). We chose values of δ_x based on the low end of the range of modern carbonate $\delta^{88/86}$Sr (0.15‰) and the highest carbonate $\delta^{88/86}$Sr we measured at Site U1468 (0.33‰). We again assume that all recrystallization adds Sr to pore fluids and is represented by the m_x term, with negligible Sr isotope exchange.

The resulting glacial seawater $\delta^{88/86}$Sr solutions given δ_x = 0.23‰ and F_x = 0.708857 have a mean of 0.32 ± 0.02‰ (95% CI), significantly lower than the modern ocean value of 0.39‰. This finding of lower glacial $\delta^{88/86}$Sr holds across the range of δ_x values assumed, except for the lowest value of 0.15‰ which results in estimated glacial seawater $\delta^{88/86}$Sr values equal to the modern value for some samples. We conclude that for the majority of reasonable scenarios capturing variability in δ_x, the estimated glacial seawater $\delta^{88/86}$Sr is lower than the modern value, corresponding to a higher-than-modern Sr inventory. In the simplest case where the recrystallized input is isotopically similar to the carbonate presently surrounding the pore fluids, we find that glacial seawater [Sr] = 98 ± 5 μM and $\delta^{88/86}$Sr = 0.32 ± 0.02‰. The effect of Sr isotopic exchange would be to shift pore fluid $\delta^{88/86}$Sr to higher values, as secondary calcite precipitation has been observed to preferentially incorporate isotopically light Sr so that progressive recrystallization leads to increasingly more ^{88}Sr-enriched pore fluids (Voigt et al., 2015). This effect requires that the fractionation between pore fluids and secondary calcite is greater than the offset between dissolving carbonates and pore fluids. In the case of such isotope exchange, the true glacial seawater $\delta^{88/86}$Sr value would be lower than the value we estimate.

4.2.3. Implications for glacial carbon cycling

Lower glacial seawater $\delta^{88/86}$Sr and higher [Sr] relative to today is expected to result from recrystallization of shallow marine carbonate exposed by sea level fall during glacial periods (Krabbenhöft et al., 2010; Paytan et al., 2021; Pearce et al., 2015; Stoll and Schrag, 1998). During the interglacial period, the re-flooding of the continental shelves cut off this Sr source while simultaneously increasing the depositional area available for shallow marine calcifiers and reef builders, which preferentially removed light Sr from the ocean reservoir and increased seawater $\delta^{88/86}$Sr to the modern value. The recycling of Sr between the shelf and seawater over glacial/interglacial cycles is tied to the long-standing "coral reef hypothesis" that describes the implications of shelf-basin partitioning of carbonate for the glacial/interglacial carbon cycle and atmospheric carbon dioxide (Berger, 1982; Opdyke and Walker, 1992; Stoll and Schrag, 1998; Walker and Opdyke, 1995). Reconstructions of deep sea carbonate burial over the last glacial cycle reveal little difference between Holocene and LGM burial rates (Cartapanis et al., 2018; Hayes et al., 2021; Wood et al., 2023), implying that the addition of alkalinity from exposed continental shelves was not compensated by lysocline deepening but instead caused excess alkalinity to temporarily build up in the global ocean during glacial periods. An increase in carbonate saturation state resulting from transient alkalinity accumulation could have additional implications for seawater $\delta^{88/86}$Sr change, with higher carbonate saturation and rates of precipitation leading to increased incorporation of light Sr isotopes in carbonate and consequently higher seawater $\delta^{88/86}$Sr (Böhm et al., 2012; Shao et al., 2021). Such saturation effects might partially counterbalance the impact of low-$\delta^{88/86}$Sr input from recrystallizing shelf carbonates, such that the reconstructed glacial seawater $\delta^{88/86}$Sr value reflects the combined, opposite effects of shelf-derived Sr input and increased kinetic fractionation.

While not definitive, our direct measurements of the contribution of preserved glacial seawater to the Maldives pore fluids suggest that the glacial carbonate weathering flux from the shelf was sufficiently large to drive a change in the ocean Sr inventory and $\delta^{88/86}$Sr despite the relatively long residence time of Sr calculated for the long-term steady state (~2 Myr). This finding adds to the accumulating evidence that seawater $\delta^{88/86}$Sr and [Sr] may have fluctuated on short (100-kyr) timescales during the Pleistocene (Krabbenhöft et al., 2010; Paytan et al., 2021; Pearce et al., 2015; Stoll and Schrag, 1998) and suggests

Table 4
Diagenetic processes and their expected influence on pore fluid Sr concentrations, stable Sr isotopes and calcium isotopes.

Process	$\delta^{88/86}$Sr fractionation	$\delta^{44/40}$Ca fractionation	Impact on pore fluid
Aragonite dissolution	$\Delta_{diss} = 0$	$\Delta_{diss} = 0$	[Sr] increase $\delta^{88/86}$Sr approaches carbonate value $\delta^{44/40}$Ca approaches carbonate value
Calcite dissolution	$\Delta_{diss} = 0$	$\Delta_{diss} = 0$	lesser [Sr] increase $\delta^{88/86}$Sr approaches carbonate value $\delta^{44/40}$Ca approaches carbonate value
Aragonite recrystallization (dissolution + secondary calcite precipitation)	Preferential incorporation of light Sr in secondary carbonate (Voigt et al., 2015) is outweighed by aragonite dissolution effect	$\Delta_{precip} = 0.0 \pm 0.1$ (Fantle and DePaolo, 2007)	[Sr] increase $\delta^{88/86}$Sr approaches carbonate value $\delta^{44/40}$Ca approaches carbonate value
Calcite recrystallization (dissolution + secondary calcite precipitation)	Preferential incorporation of light Sr in secondary carbonate (Voigt et al., 2015) dominates dissolution effect	$\Delta_{precip} = 0.0 \pm 0.1$ (Fantle and DePaolo, 2007)	lesser [Sr] increase $\delta^{88/86}$Sr increase $\delta^{44/40}$Ca approaches carbonate value
Celestine precipitation	Δ_{precip} =~-0.4 (Widanagamage et al., 2014)	n.a.	[Sr] decrease (just to maintain saturation) $\delta^{88/86}$Sr increase

that a high-resolution reconstruction of seawater $\delta^{88/86}$Sr may help constrain glacial/interglacial changes in shelf carbonate burial and recrystallization (and resulting change in global carbon and alkalinity inventories), which to this point remain difficult to quantify from observations.

4.3. Diagenetic processes impacting pore fluid $\delta^{88/86}$Sr

While the primary objective of this study was to reconstruct LGM seawater $\delta^{88/86}$Sr from the Maldives pore fluids by quantifying and subtracting away the impact of carbonate diagenesis, our data set also provides an opportunity to examine the processes that impact pore fluid Sr in shallow carbonate platform systems.

The $^{87}Sr/^{86}Sr$ profiles for both Site U1466 and Site U1468 indicate that carbonate recrystallization has altered pore fluids at all depths; progressive recrystallization of older (mainly Miocene) carbonates with depth led to decreasing pore fluid $^{87}Sr/^{86}Sr$ values relative to the modern seawater composition (Figs. 1 and 2). Because secondary carbonate incorporates less Sr than the primary phase, pore fluid [Sr] increases with progressive recrystallization; this effect is greatest for aragonite recrystallization, since aragonite incorporates ~10 times more Sr than calcite, although biogenic calcite also incorporates more Sr than inorganic forms of calcite (Zhang et al., 2020). Below 400 mbsf at Site U1468, the return towards modern seawater [Sr] despite progressively lower $^{87}Sr/^{86}Sr$ ratios could have different implications: either these pore fluids represent mixing with Holocene-age waters along with recrystallization of older sediments with lower $^{87}Sr/^{86}Sr$, or these pore fluids may be even older than the LGM, possibly from the last interglacial (MIS Stage 5e), which would give them more time to exchange Sr with surrounding Miocene-aged sediments.

The variability of pore fluid $\delta^{88/86}$Sr with depth has a more complex pattern, likely reflecting different dominant processes at different depths. The precipitation of carbonate in seawater preferentially incorporates ^{86}Sr over ^{88}Sr ($\Delta^{88/86}Sr_{carb-sw} \approx -0.18‰$) such that upon dissolution, carbonates will release isotopically light Sr to pore fluids. In addition to the reactions that occur during carbonate diagenesis, fractionation of Sr isotopes during precipitation of celestine ($SrSO_4$) may alter pore fluid $\delta^{88/86}$Sr where pore fluids become saturated with respect to $SrSO_4$ ($\Delta^{88/86}Sr_{SrSO_4-sw} \approx -0.4‰$). If pore fluids drop below celestine saturation again at greater depths, dissolution of $SrSO_4$ may provide a source of light Sr. We untangle the patterns in pore fluid $\delta^{88/86}$Sr using the context of our [Sr] and $^{87}Sr/^{86}Sr$ profiles, the mineralogy at these sites, and previously reported mass-dependent Sr isotope fractionation associated with these processes (see Table 4).

4.3.1. Site U1468 pore fluid $\delta^{88/86}$Sr

We identify four distinct intervals in the $\delta^{88/86}$Sr profile at Site U1468. In the upper 200 m, pore fluid $\delta^{88/86}$Sr decreases, approaching the value of the surrounding carbonates (Fig. 6). This trend follows the behavior of the pore fluid $^{87}Sr/^{86}Sr$, which has shifted away from the seawater composition toward the composition of the bulk carbonate due to recrystallization. The experimentally determined equilibrium Sr isotope fractionation for inorganic calcite is very close to zero ($\Delta^{88/86}Sr_{eq(carb-aq)} = -0.01 \pm 0.06‰$), suggesting that carbonate recrystallization will not measurably fractionate Sr isotopes and therefore the pore fluid $\delta^{88/86}$Sr should follow $^{87}Sr/^{86}Sr$ and approach the carbonate $\delta^{88/86}$Sr composition as recrystallization proceeds (Böhm et al., 2012). Previous work has shown this to be the case for calcium isotopes ($\Delta^{44/40}Ca_{eq(carb-aq)} \approx 0‰$) (Fantle and DePaolo, 2007; Jacobson and Holmden, 2008), and Sr is expected to behave similarly at low precipitation rates. However, Voigt et al. (2015) documented isotopically heavy $\delta^{88/86}$Sr values in deep sea carbonate sediments that were explained by fractionation during recrystallization, where secondary calcite preferentially incorporated light Sr. Consequently, we suggest that the approach of pore fluid $\delta^{88/86}$Sr toward carbonate $\delta^{88/86}$Sr within the 0–200 mbsf interval may instead be explained by the effect of aragonite dissolution "out-competing" the effect of secondary calcite precipitation during aragonite recrystallization. That is, the dissolution of aragonite has contributed so much isotopically light Sr to the pore fluids that the fractionation during calcite precipitation is insufficient to shift pore fluid $\delta^{88/86}$Sr to heavier values. This scenario may be more common in shallow marine systems where sediments are rich in aragonite, and may not commonly apply to deep sea settings where the fractionation by secondary calcite formation should dominate (Voigt et al., 2015).

At 200 mbsf, pore fluid $\delta^{88/86}$Sr reaches the lightest value observed at both our sites (0.08‰). This $\delta^{88/86}$Sr value is considerably lighter than any of the carbonates measured in this study, as well as most modern carbonates measured in other studies (Böhm et al., 2012; Krabbenhöft et al., 2010; Pearce et al., 2015). Carbonate $\delta^{88/86}$Sr values as low as 0‰ have been measured in culture experiments (Stevenson et al., 2014), but the average marine carbonate sink is ~0.15 to 0.21‰ and we have no evidence for especially low $\delta^{88/86}$Sr carbonates at this site. We hypothesize that this datum may reflect the dissolution of celestine, which was detected by X-ray diffraction at this site starting around 200 mbsf (Betzler et al., 2017). Celestine precipitates when [Sr] increases sufficiently to reach $SrSO_4$ saturation, dependent on pore fluid sulfate concentrations, with a theoretical equilibrium isotope fractionation ($\Delta^{88/86}Sr_{SrSO_4-aq}$) of approximately −0.4‰ (Widanagamage et al., 2014). If celestine precipitated from pore fluids with $\delta^{88/86}$Sr ≈ 0.24‰, its isotopic composition would be close to −0.16‰ and a small amount of dissolution could shift pore fluid $\delta^{88/86}$Sr to 0.08‰.

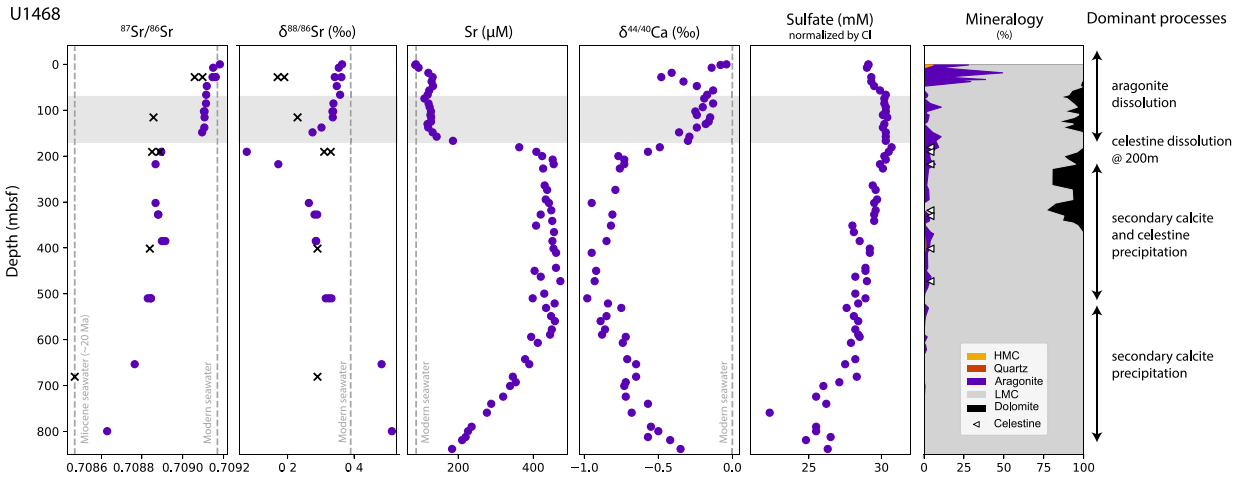

Fig. 6. Pore fluid profiles of $^{87}Sr/^{86}Sr$ and $\delta^{88/86}Sr$ from this study, with published [Sr], $\delta^{44/40}Ca$, sulfate concentrations, and sediment mineralogy for Site U1468 (Blättler et al., 2019; Betzler et al., 2017). Bulk carbonate values at select depths are plotted as black "x" symbols. The white triangles on the mineralogy plot indicate the presence of celestine ($SrSO_4$) detected by X-ray diffraction.

Between 200–500 mbsf, the increase in pore fluid $\delta^{88/86}Sr$ may be explained by multiple processes. The first possibility is that pore fluid $\delta^{88/86}Sr$ approached the $\delta^{88/86}Sr$ value of the surrounding bulk carbonate ($\Delta^{88/86}Sr_{eq(carb-aq)} = 0‰$), which is heavier (0.29–0.33‰) compared to the shallower Pleistocene/Pliocene carbonates (0.17–0.23‰). In this case, the lighter values at ~200 to 220 mbsf could be due to celestine dissolution as discussed above while the rest of the samples in this interval reflect the bulk carbonate composition. Conversely, if carbonate recrystallization instead fractionated Sr isotopes by preferentially precipitating light Sr, the shift toward higher $\delta^{88/86}Sr$ could reflect this process. Compared to the decrease in $\delta^{88/86}Sr$ above 200 mbsf where we suggest that aragonite dissolution dominated the $\delta^{88/86}Sr$ signal, secondary calcite and dolomite formation may have been the dominant process impacting $\delta^{88/86}Sr$ in this deeper interval. We favor this explanation, as it is consistent with the continuing trend of increasing $\delta^{88/86}Sr$ to values significantly greater than the bulk carbonate composition in the deepest interval (> 400 mbsf). This interpretation is also consistent with the carbonate mineralogy at this site, with the proportion of aragonite decreasing in favor of low-Mg calcite and dolomite below ~50 mbsf (Fig. 6). Additionally, pore fluid $^{87}Sr/^{86}Sr$ has achieved the same value as the bulk carbonate, [Sr] has reached a maximum, and $\delta^{44/40}Ca$ has reached the lowest values within this interval, indicating extensive recrystallization at these depths. Another process, not mutually exclusive, that could increase pore fluid $\delta^{88/86}Sr$ is the precipitation of celestine. Given that celestine was detected in sediments throughout this interval, we conclude that $SrSO_4$ precipitation may have additionally contributed to the pore fluid $\delta^{88/86}Sr$ changes. While the combined tracers point to carbonate recrystallization as the dominant process in this interval, it is not possible with the data available to deconvolve the contribution of celestine precipitation to the increasing $\delta^{88/86}Sr$ values.

Below 500 mbsf, pore fluid $\delta^{88/86}Sr$ continues to increase to values greater than both the bulk carbonate and modern seawater values. While the $^{87}Sr/^{86}Sr$, [Sr], and $\delta^{44/40}Ca$ profiles could indicate mixing with a Holocene water mass penetrating from below, consistent with the interpretations of Blättler et al. (2019), the $\delta^{88/86}Sr$ values greater than modern seawater $\delta^{88/86}Sr$ can only be explained by a process that preferentially removes light Sr isotopes from pore fluids. We take these data as evidence for fractionation during carbonate recrystallization, as previously reported by Voigt et al. (2015). Thus, we conclude that the Site U1468 $\delta^{88/86}Sr$ profile is best explained by: (1) aragonite dissolution out-competing the fractionation effect of secondary calcite formation from 0 to 200 mbsf, (2) celestine dissolution driving very light pore fluid $\delta^{88/86}Sr$ at 200 mbsf, (3) secondary calcite formation preferentially incorporating light Sr from 200 to 500 mbsf, possibly with an additive effect from precipitation of celestine (detected by X-ray diffraction in this interval), and (4) extensive secondary calcite formation further increasing pore fluid $\delta^{88/86}Sr$ below 500 mbsf (Fig. 6).

4.3.2. Site U1466 pore fluid $\delta^{88/86}Sr$

At Site U1466, where the profile covers shallower depths than Site U1468, similar carbonate recrystallization processes can explain the $\delta^{88/86}Sr$ trends. In the upper section of the profile (0 to 160 mbsf), decreasing $\delta^{88/86}Sr$ values reflect the dominant effect of aragonite dissolution on pore fluid $\delta^{88/86}Sr$. Based on our interpretation of the Site U1468 profile, we expect that fractionation of light Sr by secondary calcite precipitation has occurred in this interval but, as in the upper interval at Site U1468, this effect has been overbalanced by the release of light Sr to pore fluids from aragonite dissolution. The lowest $\delta^{88/86}Sr$ value at this site is 0.14‰, which is consistent with the range of bulk carbonate $\delta^{88/86}Sr$ and does not require a source from a phase with lower $\delta^{88/86}Sr$ (e.g., celestine, which was not detected at this site). A switch in the dominant recrystallization process explains the inflection point at 160 mbsf; below this depth the fractionation effect of secondary calcite precipitation is no longer overwhelmed by aragonite dissolution and $\delta^{88/86}Sr$ increases with depth (Fig. 7). This is consistent with the apparent minimum in pore fluid $^{87}Sr/^{86}Sr$, high [Sr], and low $\delta^{44/40}Ca$ values that are reached by 200 mbsf, indicating extensive recrystallization of carbonate.

The similarities between the Site U1466 and U1468 $\delta^{88/86}Sr$ profiles, namely decreasing values with depth to approximately 160 to 200 mbsf before $\delta^{88/86}Sr$ increases, underpins our interpretation that the two processes involved in aragonite recrystallization (aragonite dissolution, secondary calcite precipitation) are the primary drivers of these trends. Celestine dissolution/precipitation may have played a secondary role at Site U1468, but the increase in $\delta^{88/86}Sr$ for the deepest Site U1466 samples in the absence of celestine indicates that another phase must have impacted the stable Sr isotope ratios in the pore fluid. Secondary calcite is the obvious candidate, providing support for the finding of Voigt et al. (2015) that secondary calcite precipitation preferentially incorporates ^{86}Sr over ^{88}Sr leaving the pore fluids enriched in ^{88}Sr. Our results further show that the effect of this fractionation can be obscured by the effect of aragonite dissolution in young sediments, which is particularly relevant in shallow marine systems dominated by aragonite. In contrast to pore fluid calcium isotopes, where fractionation was not detected during secondary calcite precipitation and pore fluids equilibrate with the bulk carbonate $\delta^{44/40}Ca$ as recrystallization proceeds, pore fluid $\delta^{88/86}Sr$ is sensitive to the balance of aragonite dissolution and secondary calcite precipitation occurring during recrystallization.

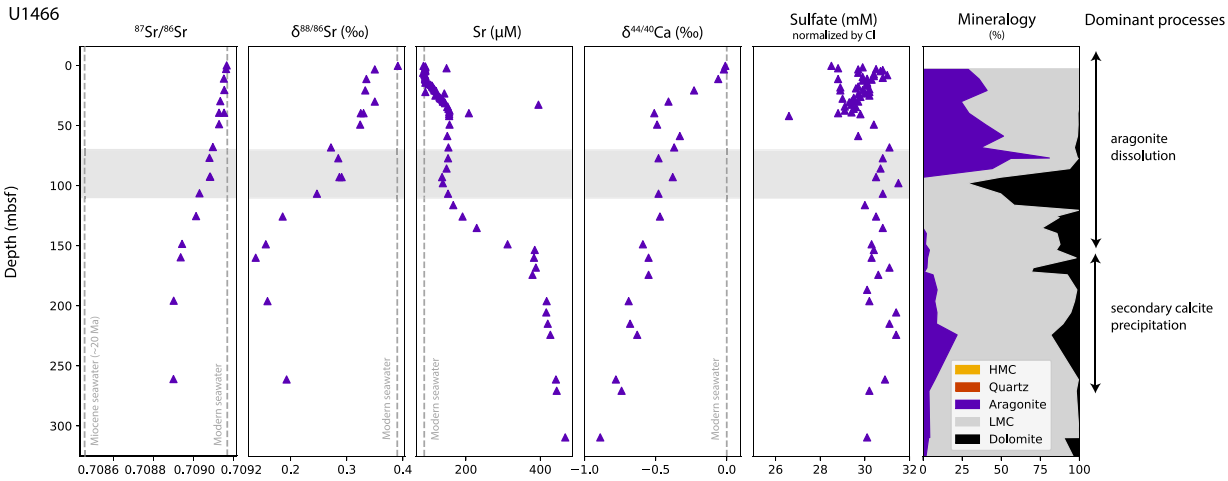

Fig. 7. Pore fluid profiles of $^{87}Sr/^{86}Sr$ and $\delta^{88/86}Sr$ from this study, with published [Sr], $\delta^{44/40}Ca$, sulfate concentrations, and sediment mineralogy for Site U1466 (Blättler et al., 2019; Betzler et al., 2017).

4.4. Bulk carbonate $\delta^{88/86}Sr$

The bulk carbonate $\delta^{88/86}Sr$ values reflect the offset from contemporaneous seawater $\delta^{88/86}Sr$ composition due to seawater-carbonate fractionation and potentially the effects of post-depositional processes that could fractionate Sr isotopes. At Site U1468, the Pleistocene/Pliocene carbonate sample (27.9 mbsf) has a $\delta^{88/86}Sr$ value consistent with the modern marine carbonate sink (0.15 to 0.21‰) (Krabbenhöft et al., 2010; Pearce et al., 2015). The deeper Miocene carbonates have significantly higher $\delta^{88/86}Sr$ values, indicating variation in seawater composition or fractionation processes occurring during or after carbonate precipitation during the Miocene compared to today. Assuming constant fractionation between seawater and carbonate through time ($\Delta^{88/86}Sr_{carb-sw} \approx -0.18$‰), the $\delta^{88/86}Sr$ values of the carbonate samples between 100 and 680 mbsf imply that early to middle Miocene seawater $\delta^{88/86}Sr$ was between 0.47 and 0.51‰, with a decrease to ~0.41‰ by the late Miocene. These inferred middle to early Miocene seawater values are significantly greater than the range of seawater $\delta^{88/86}Sr$ reconstructed by Paytan et al. (2021) for the past 35 million years, and are inconsistent with the reconstructed trend of increasing seawater $\delta^{88/86}Sr$ from a minimum of ~0.33‰ in the middle Miocene to ~0.36‰ in the late Miocene. The higher-than-expected $\delta^{88/86}Sr$ values of the carbonates between 190–680 mbsf may suggest that the seawater-carbonate fractionation factor during the Miocene was smaller than the average fractionation of carbonates in the present day ocean. Carbonate saturation state and precipitation rates have strong effects on the kinetic fractionation of Sr isotopes in calcite and, to a lesser extent, aragonite (Böhm et al., 2012; Shao et al., 2021; Stevenson et al., 2014; AlKhatib and Eisenhauer, 2017a,b). Such effects could conceivably have diminished $\Delta^{88/86}Sr_{carb-sw}$ relative to today as the global climate and carbonate system evolved throughout the Miocene, though the range of experimentally-determined $\Delta^{88/86}Sr_{aragonite-sw}$ (AlKhatib and Eisenhauer, 2017a) does not reach the small degree of fractionation implied by our measured carbonate $\delta^{88/86}Sr$ values of 0.29–0.33‰ and reconstructed seawater $\delta^{88/86}Sr$ values between 0.33 and 0.36‰. Alternatively, it is also possible that the primary $\delta^{88/86}Sr$ composition of the carbonate has since been diagenetically altered towards higher values. In a closed system, carbonate $\delta^{88/86}Sr$ is unlikely to be affected by carbonate diagenesis because carbonates contain much more Sr than pore fluids (Voigt et al., 2015). However, in a more open system with long-lived advection, evolution of pore fluid $\delta^{88/86}Sr$ to higher values through secondary calcite precipitation or celestine precipitation could drive recrystallized bulk carbonate towards higher values as well (e.g., Higgins et al., 2018; Fantle and Higgins, 2014; Ahm et al., 2018). Both mechanisms underscore the need for caution when interpreting bulk carbonate $\delta^{88/86}Sr$ values without fully understanding the potential variability of $\Delta^{88/86}Sr_{carb-sw}$ or the diagenetic history of the carbonate archive.

4.5. Geochemical and paleoceanographic implications

Our investigation of the Maldives edifice pore fluid system is the first to document variability in pore fluid $\delta^{88/86}Sr$ in a shallow marine setting. Contrary to the behavior of typical pelagic sedimentary pore fluid profiles, our results show distinct diagenetic processes dominating at different depth intervals to alter the Sr geochemistry of laterally advected water masses. Notably, while we find evidence for Sr isotope fractionation by secondary calcite formation as previously reported at pelagic sites (Voigt et al., 2015), we observe that the effect of this fractionation may be obscured by the effect of aragonite dissolution in neritic sediments during the recrystallization process. This finding indicates that early marine diagenesis in shallow marine environments may impart pore fluid signals distinct from those expected for diffusion-dominated pelagic systems, particularly where advection of water masses through much older carbonate sediments results in a high water/rock ratio, spatially variable diagenetic effects, and pore fluids that have not yet equilibrated with their host sediments. Such open-system behavior implies that diagenesis in similar platform settings has the potential to alter the chemical and isotopic composition of the primary sediment even for resistant geochemical proxies (Fantle and Higgins, 2014; Higgins et al., 2018; Ahm et al., 2018), requiring particular caution when using neritic carbonates as archives of global seawater chemistry. Broadly, this work expands our knowledge of the natural variability of the stable Sr isotope system, opening further opportunities to apply the proxy in multi-tracer investigations of early marine diagenesis.

The reconstruction of glacial seawater $\delta^{88/86}Sr$ from the Maldives pore fluids advances our understanding of the ocean Sr cycle in the past. Our results suggest that glacial seawater $\delta^{88/86}Sr$ was lower than the modern value and seawater [Sr] higher, providing new support for the evolving idea of short-term imbalances in the Sr budget (Paytan et al., 2021; Krabbenhöft et al., 2010; Stoll and Schrag, 1998; Pearce et al., 2015). The possibility of transient perturbations to the global cycle of a conservative element with a multi-million year residence time challenges the longstanding steady state paradigm (Broecker and Peng, 1982) and prompts new questions about the geological processes that may drive this short-term variability. Finally, the sedimentary $\delta^{88/86}Sr$ values from the Maldives platform might indicate a higher global carbonate burial flux $\delta^{88/86}Sr$ than previously estimated, which could help resolve the stable Sr mass balance.

5. Conclusions

The Maldives pore fluid archive presented a unique opportunity to directly constrain the $\delta^{88/86}$Sr of the glacial ocean in the preserved remnant of LGM seawater at Sites U1466 and U1468. We find that glacial seawater $\delta^{88/86}$Sr was likely lower than today (~0.32‰) and [Sr] higher (~98 μM). Our estimate is consistent with the recent proxy record that indicated the average seawater $\delta^{88/86}$Sr during the Late Quaternary was 0.35‰ (Paytan et al., 2021). These findings support the hypothesis that the glacial ocean Sr reservoir was isotopically lighter than that of the modern ocean due to shelf carbonate recrystallization during sea level regression, motivating future study of the response of seawater $\delta^{88/86}$Sr to climate-driven sea level changes on relatively short timescales.

The addition of $\delta^{88/86}$Sr to the suite of tracers measured in the Maldives pore fluids also allowed us to differentiate diagenetic processes by the fingerprint of mass-dependent fractionation, bringing new insight to the reactive histories of the distinct water masses present in this system. By documenting pore fluid $\delta^{88/86}$Sr variability in a shallow marine setting for the first time, we suggest that $\delta^{88/86}$Sr can be a useful tracer of early marine diagenesis when applied in multi-tracer studies.

CRediT authorship contribution statement

Madison M. Wood: Writing – original draft, Visualization, Methodology, Investigation, Conceptualization. **Clara L. Blättler:** Writing – review & editing, Resources, Methodology. **Ana Kolevica:** Investigation. **Anton Eisenhauer:** Resources. **Adina Paytan:** Writing – review & editing, Supervision, Methodology, Conceptualization.

Declaration of competing interest

The authors declare that they have no known competing financial interests or personal relationships that could have appeared to influence the work reported in this paper.

Acknowledgments

This research used samples and data provided by the International Ocean Discovery Program (IODP). We would like to thank the crew, technical staff, and science party of Expedition 359. This work was supported by an IODP Schlanger Ocean Drilling Fellowship and graduate student research grants from the International Association of Geochemistry and the University of California, Santa Cruz Department of Earth and Planetary Sciences (to MMW).

Data availability

Data are available through Mendeley Data at https://doi.org/10.17632/xs738ckr2m.1.

References

Ahm, A.-S.C., Bjerrum, C.J., Blättler, C.L., Swart, P.K., Higgins, J.A., 2018. Quantifying early marine diagenesis in shallow-water carbonate sediments. Geochim. Cosmochim. Acta 236, 140–159.

AlKhatib, M., Eisenhauer, A., 2017a. Calcium and strontium isotope fractionation during precipitation from aqueous solutions as a function of temperature and reaction rate; II. Aragonite. Geochim. Cosmochim. Acta 209, 320–342.

AlKhatib, M., Eisenhauer, A., 2017b. Calcium and strontium isotope fractionation in aqueous solutions as a function of temperature and reaction rate; I. Calcite. Geochim. Cosmochim. Acta 209, 296–319.

Berger, W.H., 1982. Increase of carbon dioxide in the atmosphere during deglaciation: the coral reef hypothesis. Naturwissenschaften 69 (2), 87–88.

Betzler, C., Eberli, G., Alvarez Zarikian, C., Expedition 359 Scientists, 2017. Expedition 359 summary. In: Proceedings of the International Ocean Discovery Program, vol. 359.

Betzler, C., Eberli, G.P., Lüdmann, T., Reolid, J., Kroon, D., Reijmer, J.J.G., Swart, P.K., Wright, J., Young, J.R., Alvarez-Zarikian, C., Alonso-García, M., Bialik, O.M., Blättler, C.L., Guo, J.A., Haffen, S., Horozal, S., Inoue, M., Jovane, L., Lanci, L., Laya, J.C., Hui Mee, A.L., Nakakuni, M., Nath, B.N., Niino, K., Petruny, L.M., Pratiwi, S.D., Slagle, A.L., Sloss, C.R., Su, X., Yao, Z., 2018. Refinement of Miocene sea level and monsoon events from the sedimentary archive of the Maldives (Indian Ocean). Prog. Earth Planet. Sci. 5 (1), 5.

Blättler, C.L., Higgins, J.A., Swart, P.K., 2019. Advected glacial seawater preserved in the subsurface of the Maldives carbonate edifice. Geochim. Cosmochim. Acta 257, 80–95.

Böhm, F., Eisenhauer, A., Tang, J., Dietzel, M., Krabbenhöft, A., Kisakürek, B., Horn, C., 2012. Strontium isotope fractionation of planktic foraminifera and inorganic calcite. Geochim. Cosmochim. Acta 93, 300–314.

Broecker, W.S., Peng, T.-H., 1982. Tracers in the Sea. Eldigio Press, New York.

Cartapanis, O., Galbraith, E.D., Bianchi, D., Jaccard, S.L., 2018. Carbon burial in deep-sea sediment and implications for oceanic inventories of carbon and alkalinity over the last glacial cycle. Clim. Past 14 (11), 1819–1850.

Davis, A.C., Bickle, M.J., Teagle, D.A.H., 2003. Imbalance in the oceanic strontium budget. Earth Planet. Sci. Lett. 211 (1–2), 173–187.

Fantle, M.S., DePaolo, D.J., 2006. Sr isotopes and pore fluid chemistry in carbonate sediment of the Ontong Java Plateau: Calcite recrystallization rates and evidence for a rapid rise in seawater Mg over the last 10 million years. Geochim. Cosmochim. Acta 70 (15), 3883–3904.

Fantle, M.S., DePaolo, D.J., 2007. Ca isotopes in carbonate sediment and pore fluid from ODP Site 807A: The Ca2+(aq)–calcite equilibrium fractionation factor and calcite recrystallization rates in Pleistocene sediments. Geochim. Cosmochim. Acta 71 (10), 2524–2546.

Fantle, M.S., Higgins, J.A., 2014. The effects of diagenesis and dolomitization on Ca and Mg isotopes in marine platform carbonates: Implications for the geochemical cycles of Ca and Mg. Geochim. Cosmochim. Acta 142, 458–481.

Fantle, M.S., Maher, K.M., DePaolo, D.J., 2010. Isotopic approaches for quantifying the rates of marine burial diagenesis. Rev. Geophys. 48 (3), RG3002.

Fantle, M.S., Tipper, E.T., 2014. Calcium isotopes in the global biogeochemical Ca cycle: Implications for development of a Ca isotope proxy. Earth-Sci. Rev. 129, 148–177.

Fietzke, J., Eisenhauer, A., 2006. Determination of temperature-dependent stable strontium isotope (88Sr/86Sr) fractionation via bracketing standard MC-ICP-MS. Geochem. Geophys. Geosyst. 7 (8), Q08009.

Geske, A., Lokier, S., Dietzel, M., Richter, D., Buhl, D., Immenhauser, A., 2015. Magnesium isotope composition of sabkha porewater and related (Sub-)Recent stoichiometric dolomites, Abu Dhabi (UAE). Chem. Geol. 393–394, 112–124.

Hayes, C.T., Costa, K.M., Anderson, R.F., Calvo, E., Chase, Z., Demina, L.L., Dutay, J.-C., German, C.R., Heimbürger-Boavida, L.-E., Jaccard, S.L., Jacobel, A., Kohfeld, K.E., Kravchishina, M.D., Lippold, J., Mekik, F., Missiaen, L., Pavia, F.J., Paytan, A., Pedrosa-Pamies, R., Petrova, M.V., Rahman, S., Robinson, L.F., Roy-Barman, M., Sanchez-Vidal, A., Shiller, A., Tagliabue, A., Tessin, A.C., Hulten, M.v., Zhang, J., 2021. Global ocean sediment composition and burial flux in the deep sea. Glob. Biogeochem. Cycles 35 (4), e2020GB006769.

Henderson, G.M., Martel, D.J., O'Nions, R.K., Shackleton, N.J., 1994. Evolution of seawater 87Sr/86Sr over the last 400 ka: the absence of glacial/interglacial cycles. Earth Planet. Sci. Lett. 128, 643–651.

Higgins, J.A., Blättler, C., Lundstrom, E., Santiago-Ramos, D., Akhtar, A., Crüger Ahm, A.-S., Bialik, O., Holmden, C., Bradbury, H., Murray, S., Swart, P., 2018. Mineralogy, early marine diagenesis, and the chemistry of shallow-water carbonate sediments. Geochim. Cosmochim. Acta 220, 512–534.

Higgins, J.A., Schrag, D., 2012. Records of Neogene seawater chemistry and diagenesis in deep-sea carbonate sediments and pore fluids. Earth Planet. Sci. Lett. 357–358, 386–396.

Jacobson, A.D., Holmden, C., 2008. δ^{44}Ca evolution in a carbonate aquifer and its bearing on the equilibrium isotope fractionation factor for calcite. Earth Planet. Sci. Lett. 270 (3–4), 349–353.

Krabbenhöft, A., Eisenhauer, A., Böhm, F., Vollstädt, H., Fietzke, J., Liebetrau, V., Augustin, N., Peucker-Ehrenbrink, B., Müller, M.N., Horn, C., Hansen, B.T., Nolte, N., Wallmann, K., 2010. Constraining the marine strontium budget with natural strontium isotope fractionations (^{87}Sr/^{86}Sr*, $\delta^{88/86}$Sr) of carbonates, hydrothermal solutions and river waters. Geochim. Cosmochim. Acta 74 (14), 4097–4109.

Krabbenhöft, A., Fietzke, J., Eisenhauer, A., Liebetrau, V., Böhm, F., Vollstädt, H., 2009. Determination of radiogenic and stable strontium isotope ratios (^{87}Sr/^{86}Sr, $\delta^{88/86}$Sr) by thermal ionization mass spectrometry applying an ^{87}Sr/^{84}Sr double spike. J. Anal. At. Spectrom. 24 (9), 1267–1271.

McArthur, J.M., Howarth, R.J., Shields, G.A., Zhou, Y., 2020. Chapter 7 - Strontium isotope stratigraphy. In: Gradstein, F.M., Ogg, J.G., Schmitz, M.D., Ogg, G.M. (Eds.), Geologic Time Scale 2020. Elsevier, pp. 211–238.

Mokadem, F., Parkinson, I.J., Hathorne, E.C., Anand, P., Allen, J.T., Burton, K.W., 2015. High-precision radiogenic strontium isotope measurements of the modern and glacial ocean: Limits on glacial-interglacial variations in continental weathering. Earth Planet. Sci. Lett. 415, 111–120.

Opdyke, B.N., Walker, J.C.G., 1992. Return of the coral reef hypothesis: Basin to shelf partitioning of CaCO3 and its effect on atmospheric CO2. Geology 20 (8), 733–736.

Paytan, A., Griffith, E.M., Eisenhauer, A., Hain, M.P., Wallmann, K., Ridgwell, A., 2021. A 35-million-year record of seawater stable Sr isotopes reveals a fluctuating global carbon cycle. Science 371 (6536), 1346–1350.

Pearce, C.R., Parkinson, I.J., Gaillardet, J., Charlier, B.L.A., Mokadem, F., Burton, K.W., 2015. Reassessing the stable ($\delta^{88/86}$Sr) and radiogenic (^{87}Sr/^{86}Sr) strontium isotopic composition of marine inputs. Geochim. Cosmochim. Acta 157, 125–146.

Richter, F.M., DePaolo, D.J., 1987. Numerical models for diagenesis and the Neogene Sr isotopic evolution of seawater from DSDP Site 590B. Earth Planet. Sci. Lett. 83 (1), 27–38.

Richter, F.M., DePaolo, D.J., 1988. Diagenesis and Sr isotopic evolution of seawater using data from DSDP 590B and 575. Earth Planet. Sci. Lett. 90 (4), 382–394.

Riechelmann, S., Mavromatis, V., Buhl, D., Dietzel, M., Eisenhauer, A., Immenhauser, A., 2016. Impact of diagenetic alteration on brachiopod shell magnesium isotope (δ^{26}Mg) signatures: Experimental versus field data. Chem. Geol. 440, 191–206.

Shao, Y., Farkaš, J., Mosley, L., Tyler, J., Wong, H., Chamberlayne, B., Raven, M., Samanta, M., Holmden, C., Gillanders, B.M., Kolevica, A., Eisenhauer, A., 2021. Impact of salinity and carbonate saturation on stable Sr isotopes ($\delta^{88/86}$Sr) in a lagoon-estuarine system. Geochim. Cosmochim. Acta 293, 461–476.

Stevenson, E.I., Hermoso, M., Rickaby, R.E.M., Tyler, J.J., Minoletti, F., Parkinson, I.J., Mokadem, F., Burton, K.W., 2014. Controls on stable strontium isotope fractionation in coccolithophores with implications for the marine Sr cycle. Geochim. Cosmochim. Acta 128, 225–235.

Stoll, H.M., Schrag, D.P., 1998. Effects of Quaternary sea level cycles on strontium in seawater. Geochim. Cosmochim. Acta 62 (7), 1107–1118.

Stoll, H.M., Schrag, D.P., Clemens, S.C., 1999. Are seawater Sr/Ca variations preserved in Quaternary foraminifera? Geochim. Cosmochim. Acta 63 (21), 3535–3547.

Turchyn, A.V., DePaolo, D.J., 2011. Calcium isotope evidence for suppression of carbonate dissolution in carbonate-bearing organic-rich sediments. Geochim. Cosmochim. Acta 75 (22), 7081–7098.

Vance, D., Teagle, D.A.H., Foster, G.L., 2009. Variable Quaternary chemical weathering fluxes and imbalances in marine geochemical budgets. Nature 458 (7237), 493–496.

Voigt, J., Hathorne, E.C., Frank, M., Vollstaedt, H., Eisenhauer, A., 2015. Variability of carbonate diagenesis in equatorial Pacific sediments deduced from radiogenic and stable Sr isotopes. Geochim. Cosmochim. Acta 148, 360–377.

Walker, J.C.G., Opdyke, B.C., 1995. Influence of variable rates of neritic carbonate deposition on atmospheric carbon dioxide and pelagic sediments. Paleoceanography 10 (3), 415–427.

Widanagamage, I.H., Schauble, E.A., Scher, H.D., Griffith, E.M., 2014. Stable strontium isotope fractionation in synthetic barite. Geochim. Cosmochim. Acta 147, 58–75.

Wood, M., Hayes, C.T., Paytan, A., 2023. Global Quaternary carbonate burial: Proxy- and model-based reconstructions and persisting uncertainties. Annu. Rev. Mar. Sci. 15 (1), 277–302.

Zhang, S., Zhou, R., DePaolo, D.J., 2020. The seawater Sr/Ca ratio in the past 50 Myr from bulk carbonate sediments corrected for diagenesis. Earth Planet. Sci. Lett. 530, 115949.